First-principles investigation on the structural, elastic, electronic and optical properties and possible mechanism of the photocatalytic properties for orthorhombic and tetragonal KNbO₃

Yong-Qiang Xu[a,b,*], Shao-Yi Wu[a,**], Li-Na Wu[a], Li-Juan Zhang[a]

[a] Department of Applied Physics, School of Physical Electronics, University of Electronic Science and Technology of China, Chengdu 610054, PR China
[b] College of Physics and Electronic Information, Gannan Normal University, Ganzhou 341000, PR China

ARTICLE INFO

ABSTRACT

The structural, elastic, electronic, optical and photocatalytic properties are studied for orthorhombic and tetragonal KNbO₃ (KNO) based on first-principles methods. The elastic results show that both phases are mechanically stable, and the tetragonal phase exhibits higher hardness and stiffness than the orthorhombic one. The elastic properties also exhibit obvious elastic anisotropy in both crystals. The electronic structures with HSE06 scheme show that both systems are indirect band gap semiconductors, and the Nb-O bonds in tetragonal phase have stronger covalency than those in orthorhombic phase. The optical properties are also calculated with HSE06 method. The complex dielectric function and linear optical properties are discussed in detail. The significant optical anisotropy is observed in (001) direction of tetragonal phase. Then the mechanisms of photocatalytic properties of both polymorphs are further discussed and compared. From the present band structures, the effective mass of photogenerated carriers and optical absorption spectra results, the photocatalytic activity of orthorhombic phase can be higher than the tetragonal one.

1. Introduction

Potassium niobate KNbO₃ (KNO) is a well-known ABO₃ type perovskite oxide which possesses attractive physical properties such as large electro-optic coefficients [1,2], large nonlinear optical coefficients [2–4] and high photocatalytic activity [5–7] as well as ferroelectricity [8,9] and piezoelectric anisotropy [10,11]. The crystal structure of KNO has mainly cubic, tetragonal, orthorhombic and rhombohedral phases under different synthetic conditions, showing a sequence of structural phase transformations with temperature and pressure [12–16]. Meanwhile, KNO is also a promising water-splitting photocatalyst [5–7,17]. It can also be used as a potential ferroelectric material under tetragonal, orthorhombic and rhombohedral phases, e.g., K₁₋ₓNaₓNbO₃ alloy as the important alterative for PbZrₓTi₁₋ₓO₃ (PZT) alloy due to its non-toxicity [18,19].

In view of its important applications, considerable efforts have been made to reveal the physical properties of KNO in different phases in recent decades, and many excellent theoretical [20–30] and experimental [31–35] results have been obtained so far. Due to the fundamental and practical significance, the elasticity, electronic structures and optical properties have been concerned partially for KNO [36–43].

Nevertheless, there are still many important aspects that need to be further investigated. First, to the best of our knowledge, previous theoretical studies for the physical properties of KNO largely focus on the cubic phase, whereas little attention has been paid on the orthorhombic and tetragonal phases. Particularly, the important information about elastic anisotropy, mechanism properties, Debye temperature, linear optical properties, etc. is still insufficient for orthorhombic and tetragonal KNO (O- and T-KNO) and needs to be improved or supplemented. Second, previous results were mainly based on the conventional density functional theory with local density approximation (LDA) or generalized gradient approximation (GGA) [36–43], which could indeed provide reasonable results for relative study. However, these methods are much less accurate with regard to the electronic and optical properties due to the omission of the contributions from quasiparticle renormalization of electronic band gaps, thermal effects owing to the electron-phonon coupling and excitonic effects in the linear and nonlinear optical absorption [30]. Therefore, these results for KNO could be further improved by using some innovative and more advanced calculational schemes such as HSE06 so as to provide more accurate electronic structures and optical properties which are also useful to deepen the researches of its photoactivity. Third, the comparison between O-

and T-KNO has been quite scarce up to now. Since the structural, elastic, electronic and optical properties of KNO can change accordingly under different symmetries, the above comparison is worthy to be performed in a systematical way. Finally, as a promising photocatalyst, the photocatalytic mechanisms of O- and T-KNO has not been discussed and compared in detail so far, which deserve to be further investigated.

Under such circumstance, to fully understand the relevant physical properties of O- and T-KNO, a relatively comprehensive theoretical investigation and comparison of the structural, elastic, electronic and optical properties is performed in this work. The aim of this paper is to present the results of a theoretical investigation of O- and T-KNO on the basis of first-principles methods, which would be helpful for the understanding of phase transitions, band gap tunability and photocatalytic applications of KNO crystals.

2. Computational methods

All the calculations are performed with Vienna *Ab initio* Simulation Package (VASP) [44–46]. The electron-ion interaction is described by the projector augmented wave (PAW) potentials [47]. The electronic configurations used for calculations are $3s^23p^64s^1$ for K, $4p^64d^45s^1$ for Nb, and $2s^22p^4$ for O. The electronic wave functions are expanded into plane waves up to a kinetic energy of 500 eV for whole calculations. All structural degrees of freedom are relaxed until the forces on each atom are below 1 meV/Å. The Brillouin-zone integrations are performed using a shifted Monkhorst- Pack $8 \times 8 \times 8$ and $7 \times 11 \times 7$ k-point mesh for tetragonal and orthorhombic phases, respectively. For geometric structure optimization, four different functions, i.e., LDA of Ceperley-Adler [48], GGA of Perdew-Burke-Ernzerhof (PBE) [49], PBEsol [50] and Heyd-Scueria-Ernzerhof (HSE06) [51] functionals are employed to describe the electronic exchange-correlation interactions. After both crystals are fully relaxed to attain the equilibrium geometries, the elastic tensor is further calculated based on the relaxed structures. The elastic constants are derived from the stress-strain [52] relationship with LDA, PBE, and PBEsol schemes. Electronic structure and optical properties calculations are performed by using HSE06 scheme, which can offer a more reliable and rigorous band-structure calculation within the framework of quasiparticle theory and may effectively overcome the band gap problem of conventional DFT calculations with local or semilocal exchange-correlation functions.

3. Results and discussion

3.1. Structural properties

KNO is orthorhombic symmetry at ambient temperature with space group Bmm2 with ten atoms in the unit cell, exhibiting ferroelectricity. The experimental lattice parameters are about $a = 5.695$ Å, $b = 3.973$ Å and $c = 5.721$ Å for O-KNO [9]. T-KNO with space group $P4mm$ ($a \approx b \approx 3.997$ Å, $c \approx 4.063$ Å [9]) has slight elongation distortion along c axis in comparison to cubic KNO with space group $Pm\bar{3}m$ and experimental lattice constant $a_0 \approx 4.022$ Å [53]. Fig. 1 shows the unit cell of T- and O-KNO using VESTA software [54].

In order to obtain equilibrium geometry, the total energy as a function of volume is calculated by using four functions (LDA, PBE, PBEsol and HSE06) for the above two polymorphs. The obtained
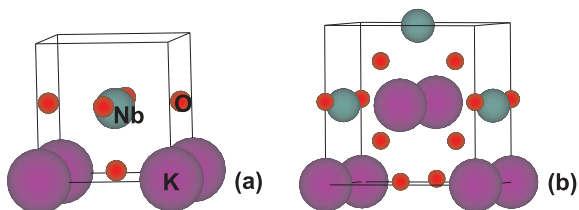

Fig. 1. The unit cell of tetragonal (a) and orthorhombic (b) $KNbO_3$.

Table 1
The calculated lattice parameters a, b and c (in Å), bulk modulus B_0 (in GPa) and its pressure derivative B' of O- and T-KNO with LDA, PBE, PBEsol and HSE06 functions.

			a	b	c	B_0	B'
O-KNO							
	Present	LDA	5.657	3.975	5.666	181.13	4.67
		PBE	5.823	4.016	5.860	163.69	4.51
		PBEsol	5.724	4.001	5.740	167.39	4.54
		HSE06	5.719	3.972	5.748	187.65	4.54
	Theoretical	GGA	5.744[a]	3.980[a]	5.771[a]		
	Experimental		5.695[b]	3.973[b]	5.721[b]		
			5.695[c]	3.971[c]	5.720[c]		
			5.641[d]	4.002[d]	5.721[d]		
			5.697[e]	3.971[e]	5.721[e]		
			5.697[f]	3.971[f]	5.722[f]		
T-KNO							
	Present	LDA	3.979	3.979	4.021	182.79	4.35
		PBE	4.026	4.026	4.225	159.19	4.15
		PBEsol	4.008	4.008	4.083	170.37	4.25
		HSE06	3.995	3.995	4.061	189.83	4.23
	Theoretical	LDA	3.950[g]	3.950[g]	3.983[g]		
		LDA	3.945[h]	3.945[h]	3.989[h]		
		PBE	3.994[h]	3.994[h]	4.193[h]		
		PBE	3.984[i]	3.984[i]	4.146[i]		
		PBEsol	3.969[h]	3.969[h]	4.058[h]		
		GGA	3.992[a]	3.992[a]	4.128[a]		
	Experimental		3.997[b]	3.997[b]	4.063[b]		

^a Ref. [29].
^b Ref. [9].
^c Ref. [31].
^d Ref. [32].
^e Ref. [57].
^f Ref. [58].
^g Ref. [40].
^h Ref. [30].
ⁱ Ref. [56].

energy-volume dependences $E = E(V)$ are fitted to three-order Birch-Murnaghan equation of states (BM3-EOS) [55] to obtain the equilibrium lattice constants a, b and c, the bulk modulus B_0, and the pressure derivative B'. The relevant parameters are summarized in Table 1, together with some theoretical results [29,30,40,56] and the available experimental data [9,31,32,57,58] for comparison. From Table 1, it is easy to see that LDA and PBE underestimate and overestimate the lattice constants, respectively, while the results from PBEsol and HSE06 are in good agreement with the available experimental values for both polymorphs. Which confirm the validity and reliability of the performed calculations. Further, the bulk modulus B_0 obtained from the experimental elastic constant [58] ($\approx$ 172.89 GPa) also substantially supports the present fitting result from BM3-EOS for O-KNO.

3.2. Elastic properties

3.2.1. Elastic constants and mechanical properties

Abundant mechanical information of materials is included in the elastic constants. Generally, elastic stiffness tensor has 21 non-zero independent elements which can be further reduced under higher symmetries [59]. Specifically, there are six (C_{11}, C_{12}, C_{13}, C_{33}, C_{44} and C_{66}) and nine (C_{11}, C_{12}, C_{13}, C_{22}, C_{23}, C_{33}, C_{44}, C_{55} and C_{66}) independent elastic constants for present T- and O-KNO single crystal, respectively. Based on the fully relaxed structures, the elastic constants are obtained for both polymorphs using LDA, PBE, and PBEsol schemes. The corresponding results are tabulated in Table 2, together with other available theoretical and experimental data [29,58,60–62] for comparison. From Table 2, present elastic constants obtained with LDA and PBEsol are suitably consistent with the experimental results [58,60,61] for O-KNO. Despite absence of experimental elastic constants for T-KNO, those obtained with PBEsol are in accordance with the previous theoretical values [29]. Meanwhile, the present elastic constants satisfy